Available online at www.sciencedirect.com
ScienceDirect
Computers and Mathematics with Applications 55 (2008) 2903–2912
An International Journal
computers & mathematics with applications
www.elsevier.com/locate/camwa

Buoyancy convection in a cavity with mutually orthogonal heated plates

S. Saravanan[a,*], A.K. Abdul Hakeem[a], P. Kandaswamy[b], J. Lee[b]

[a] *UGC-DRS Center for Fluid Dynamics, Department of Mathematics, Bharathiar University, Coimbatore 641 046, India*
[b] *School of Mechanical Engineering, Yonsei University, Seoul, Republic of Korea*

Received 25 June 2007; received in revised form 5 September 2007; accepted 17 November 2007

Abstract

Buoyancy driven convection in a square cavity induced by two mutually orthogonal arbitrarily placed heated thin plates is studied numerically under isothermal and isoflux boundary conditions. The flow is assumed to be two-dimensional. The coupled governing equations were solved by the finite difference method using the Alternating Direction Implicit technique and Successive Over Relaxation method. The steady state results are depicted in terms of streamline and isotherm plots. It is found that the resulting convection pattern is stronger for the isothermal boundary condition. A better overall heat transfer can be achieved by placing one of the plates far away from the center of the cavity for isothermal boundary condition and near the center of the cavity for isoflux boundary condition.

Keywords: Buoyancy; Cavity; Isothermal; Isoflux; Natural convection

1. Introduction

Heat transfer in sealed cavities arising from buoyancy induced natural convection is an important mechanism for several physical systems. Simple cavities defined as single chambers with no obstructions in them have been extensively studied in the past few decades (see [1–5]). The current interest has now shifted to complex cavities containing obstruction or partitions which have important implications in many branches of engineering particularly in the microelectronics fabrication industry. The continued miniaturization of high dense integrated circuits associated with increased heat dissipation has made an effective natural convection cooling of electronic components mandatory. Hence a number of convection studies both numerical and experimental are being conducted in this aspect.

Natural convection studies within a laterally heated two-dimensional partitioned rectangular cavity with adiabatic top and bottom walls have been extensively reported. Bajorek and Lloyd [6] made an experimental investigation on a cavity with partitions protruding centrally from the top and bottom adiabatic walls. Later Ciofalo and Karayiannis [7] made a numerical simulation for this setup. The effect of mounting a partial partition of zero thickness on the lateral active cold wall was analyzed by Fredrick [8]. In all these studies the partitions caused convection suppression and

* Corresponding author. Tel.: +91 422 2422222x415; fax: +91 422 2425706.
E-mail address: sshravan@lycos.com (S. Saravanan).

0898-1221/$ - see front matter © 2007 Elsevier Ltd. All rights reserved.
doi:10.1016/j.camwa.2007.11.024

Nomenclature

d_1	distance between center of cavity and the horizontal plate (m)
D_1	dimensionless distance $= d_1/\mathrm{L}$
d_2	distance between center of cavity and the vertical plate (m)
D_2	dimensionless distance $= d_2/\mathrm{L}$
g	acceleration due to gravity (m/s^2)
Gr	Grashof number $= g\beta(\theta_h - \theta_c)L^3/\nu^2$
H	height of the cavity (m)
L	length of the cavity (m)
Nu	local Nusselt number $= \partial T/\partial X_i$ for ITBC $q''L/k(T_h - T_c)$ for IFBC
Nu_{wall}	average Nusselt number $= \int_{-0.5}^{0.5} Nu \, \mathrm{d}X_i$
$\overline{Nu}$	average Nusselt number
P	Pressure (Pa)
Pr	Prandtl number $= \nu/\alpha$
t	time (s)
T	dimensionless temperature
v_1	vertical velocity (m/s)
V_1	dimensionless vertical velocity
v_2	horizontal velocity (m/s)
V_2	dimensionless horizontal velocity
x_1	vertical coordinate (m)
X_1	dimensionless vertical coordinate
x_2	horizontal coordinate (m)
X_2	dimensionless horizontal coordinate
α	thermal diffusivity of fluid (m^2/s)
β	volumetric coefficient of expansion of fluid (1/K)
θ	temperature (K)
ψ	stream function (m^2/s)
μ	dynamic viscosity of fluid (Pa.s)
ν	kinematic viscosity of fluid $= \mu/\rho$ (m^2/s)
ρ	density of fluid (kg/m^3)
τ	dimensionless time
ω	vorticity (1/s)
Ψ	dimensionless stream function
ζ	dimensionless vorticity

Subscript

c	cold
h	hot

heat transfer reduction. Modification of heat transfer in cavities due to the introduction of isothermal fins has also received considerable attention. Shi and Khodadadi [9] and Lakhal et al. [10] have discussed the influence of adding isothermal fins to one of the active walls. They identified flow patterns modified by the hydrodynamic blockage effect depending on the length of the fin and an extra heating of the fluid that is offered by the fin. Moreover the extra heating mechanism offset the hydrodynamic blockage effect and contributed to the strengthening of the flow field for high Rayleigh numbers. Conjugate conduction convection in differentially heated cavities containing a conducting or heat generating solid block is also found in the literature (see [11–13]). It was found that the heat transfer across the cavities can be adjusted by changing the physical and geometrical constraints. Another problem of interest is to extract heat from hotter bodies contained in closed cavities. Oztop et al. [14] have addressed such an issue with a thin heated

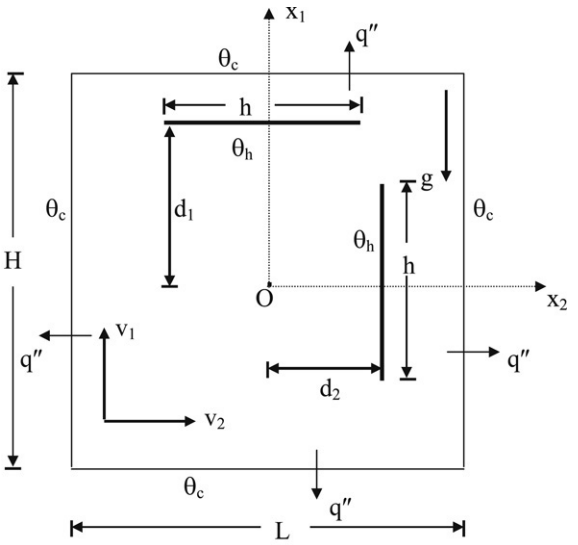

Fig. 1. Physical configuration.

plate built in vertically or horizontally and found that heat transfer is enhanced about 20% when the plate is located vertically. Dagtekin and Oztop [15] have dealt with the heat removal from two heated vertical partitions of different heights placed on the bottom of a cavity and observed the enhancement of heat transfer with an increase in spacing between the two partitions.

Natural convection in cavities with constant flux has been studied by many authors. Natural convection in a square cavity with a discrete heat source for different boundary conditions with isoflux discrete heat source and isothermal discrete heat source was analyzed numerically by Ahmed and Yovanovich [16]. Milanez [17] performed the numerical study of steady natural convection in a rectangular enclosure heated from below and cooled from the sides. They observed that, for the square cavity, the flow and thermal fields are not strongly affected by the isothermal or constant heat flux boundary condition at the bottom heat source. Recently, Sharif and Mohammad [18] performed a numerical study of natural convection in a rectangular cavity with constant flux at the bottom and symmetrically cooled from the vertical walls. They found that at lower Grashof number, diffusion is the dominating heat transfer mechanism whereas at higher Grashof number buoyancy convection is dominating.

Heat transfer in cavities with heating elements mounted in a mutually orthogonal fashion has received limited attention though such configurations are frequently encountered in the microelectronics industry. Papanicolaou and Jaluria [19] and Icoz and Jaluria [20] have considered similar cases in their design and optimization of cooling systems for electronic equipments. Keeping this in mind this paper deals with a numerical study of heat transfer in a cavity with two mutually orthogonal heating elements for two different boundary conditions, viz., isothermal boundary condition (ITBC) and isoflux boundary condition (IFBC). This type of configuration models one of the simplest cases and enables one to study the relative location of a heating element with respect to the other.

2. Mathematical analysis

The configuration under consideration is shown schematically in Fig. 1. It is a square cavity of height H and length L with two mutually orthogonal isothermally heated thin plates, each of length $L/2$. The plates are placed in such a way that they are parallel to the walls of the cavity. The horizontal and vertical plates are at distances d_1 and d_2 respectively from the center O of the cavity. All the four walls of the cavity are isothermally maintained at a constant temperature θ_c which is lower than that of the heated plates for ITBC and a uniform outward heatflux q'' is applied at the walls for IFBC. The cartesian coordinates (x_1, x_2) with the corresponding velocity components (v_1, v_2) are chosen. The gravity g acts downwards normal to the x_2 direction.

The nondimensional equations governing the laminar two-dimensional incompressible flow of the fluid under the Oberbeck–Boussinesq approximation [21] in an environment described above are

$$\frac{\partial \zeta}{\partial \tau} - \frac{\partial \psi}{\partial X_2}\frac{\partial \zeta}{\partial X_1} + \frac{\partial \psi}{\partial X_1}\frac{\partial \zeta}{\partial X_2} = Gr\frac{\partial T}{\partial X_2} + \nabla^2 \zeta \tag{1}$$

$$\frac{\partial T}{\partial \tau} - \frac{\partial \psi}{\partial X_2}\frac{\partial T}{\partial X_1} + \frac{\partial \psi}{\partial X_1}\frac{\partial T}{\partial X_2} = \frac{1}{Pr}\nabla^2 T \tag{2}$$

$$\nabla^2 \psi = -\zeta \tag{3}$$

$$\text{where } V_1 = -\frac{\partial \psi}{\partial X_2}, \qquad V_2 = \frac{\partial \psi}{\partial X_1} \quad \text{and} \quad \zeta = \frac{\partial V_1}{\partial X_2} - \frac{\partial V_2}{\partial X_1}. \tag{4}$$

The nondimensional parameters that appear in the equations are

$$X_1 = \frac{x_1}{L}, \qquad X_2 = \frac{x_2}{L}, \qquad V_1 = \frac{v_1}{\nu/L}, \qquad V_2 = \frac{v_2}{\nu/L}, \qquad \tau = \frac{t}{L^2/\nu},$$

$$T = \frac{\theta - \theta_c}{\theta_h - \theta_c} \quad \text{for ITBC}, \qquad T = \frac{(\theta - \theta_c)k}{q''L} \quad \text{for IFBC}$$

$$\Psi = \frac{\psi}{\nu}, \qquad \zeta = \frac{\omega}{\nu/L^2}, \qquad \text{the Grashof number } Gr = \frac{g\beta(\theta_h - \theta_c)L^3}{\nu^2} \quad \text{and}$$

$$\text{the Prandtl number } Pr = \frac{\nu}{\alpha}. \tag{5}$$

The initial and boundary conditions in the dimensionless form are:

$$\tau = 0: \quad V_i = 0; \qquad T = 0; \qquad -\frac{1}{2} \le X_i \le \frac{1}{2} \tag{6}$$

$$\tau > 0: \quad V_i = 0; \qquad T = 0; \qquad X_i = \pm\frac{1}{2} \quad \text{for ITBC} \tag{7}$$

$$V_i = 0; \qquad \frac{\partial T}{\partial X_i} = \pm 1; \qquad X_i = \pm\frac{1}{2} \quad \text{for IFBC} \tag{8}$$

$$V_i = 0; \qquad T = 1 \quad \text{on the plates } (i = 1, 2). \tag{9}$$

In order to measure the heat transfer rate in the cavity, it is necessary to define wall Nusselt numbers at the four walls as $Nu_{\text{wall}} = \int_{-0.5}^{0.5} Nu \mathrm{d}X_i$, where the local Nusselt number

$$Nu = \begin{cases} \dfrac{\partial T}{\partial X_i} & \text{for ITBC and} \\ \dfrac{1}{T} & \text{for IFBC.} \end{cases}$$

The average Nusselt number $\overline{Nu}$ is then calculated by averaging the wall Nusselt numbers at the four walls. If one of the heat generating plates lies on a cavity wall, only the remaining part of that wall is taken into account in calculating Nu_{wall}.

The motion of the liquid governed by the continuity, momentum and energy equations are solved numerically using the finite difference method with a regular cartesian space grid. An Alternating Direction Implicit (ADI) technique and Successive Over Relaxation (SOR) method are employed to solve the discretized equations as reported in [5]. The results obtained by the code developed were validated against those of Zhong et al. [3] and Oztop et al. [14] for ITBC and Sharif et al. [18] for IFBC (see Fig. 2(b)). In both the cases we observe a good agreement. In order to determine a proper grid size for this study, a grid independency test was conducted for $Gr = 10^6$, $Pr = 0.71$ and $D_1 = D_2 = 0$. Five different grids 41×41, 61×61, 81×81, 101×101 and 121×121 were chosen. The maximum value of the stream function of the primary eddy ($\Psi_{\max}$) was used as a sensitivity measure of the accuracy of the solution. Fig. 2(a) shows that the two grids 101×101 and 121×121 give nearly identical results. Hence considering both the accuracy and the computational time, the computations were all performed with a 101×101 grid.

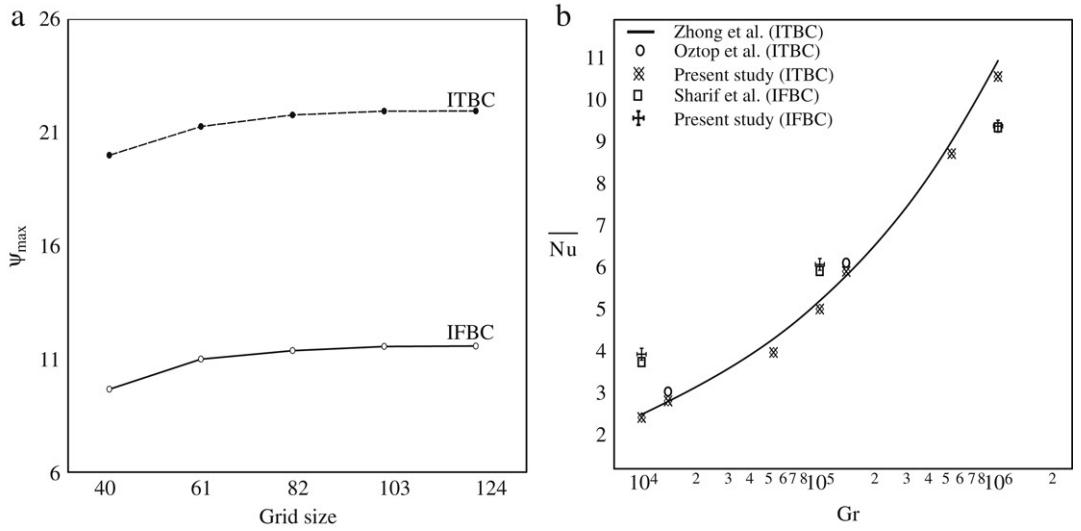

Fig. 2. (a) $\Psi_{\max}$ as a function of the grid size. (b) Correlation of present numerical results with others.

3. Results and discussion

Natural convection in a square cavity due to two mutually orthogonal arbitrarily placed heated thin plates is investigated numerically for ITBC and IFBC. The computations were carried out for $Pr = 0.71$, corresponding to air and $Gr = 10^6$. Isotherms and streamline counters were plotted for eight and five equally spaced values between $T_{\min}$ and $T_{\max}$ for temperature and zero and $\Psi_{\max}$ for the stream function respectively throughout the study. When $D_2 = 0$, the problem is symmetric about $X_2 = 0$. Hence we have presented both isotherms and streamlines in a single plot to study the effect of different locations of the horizontal plate. When $D_1 = 0$, the problem is anti-symmetric about $X_2 = 0$. Hence we have considered only the positive values of D_2 in studying the effect of vertical plate movement.

3.1. Isothermal boundary condition (ITBC)

The isotherms and streamlines for various positions of the horizontal plate are displayed in Fig. 3 when $D_2 = 0$. They clearly indicate two counter-rotating moderate convection cells both rising at the center of the cavity. Each cell has a stronger primary eddy at the top and weaker secondary eddy at the bottom of the cavity for $D_1 = 0 = D_2 = 0$. When the horizontal plate is moved upward to $D_1 = 0.125$, a decrease in the strength of the primary eddy is observed as expected. Further, upward movement to $D_1 = 0.25$ of the plate affects the flow characteristics significantly. The plate acts as a mechanical barrier and retards the convection cells to develop above it, i.e., it suppresses the primary eddy. The corresponding changes in the shape of the isotherms above the plate support this. Thus a further reduction in $\Psi_{\max}$ is observed. When the plate moves more closer ($D_1 = 0.375$) to the wall, conduction becomes more prominent above the plate accompanied by flat isotherms which is an expected result, hence the graph is not displayed. This forces a weak secondary eddy to grow and occupy the remaining half of the cavity. When $D_1 = 0.5$ (wall mounted case), two weaker convection cells occupy the entire cavity. Thus, the upward movement of the horizontal plate from the center to the top of the cavity suppresses the primary eddies and hence leads to the development of the secondary eddies.

A similar explanation holds good when the plate moves in the downward direction. Here the downward movement of the plate from the center to the bottom of the cavity suppresses the secondary vortices and paves the way for the primary eddies to grow and occupy the entire cavity. Thus the negative values of D_1 correspond to more efficient heat transfer compared to its positive values. From Fig. 6(a) in general (except the cases $D_1 = 0.375$ and $D_1 = -0.375$), we observe that $\overline{Nu}$ decreases as the horizontal plate moves from the bottom to the top of the cavity. This is because of the adverse temperature gradient responsible for the unstable situation, when the plate is near the bottom. When $D_1 = 0.375$ and -0.375, we observe a slight increase in $\overline{Nu}$. This may be due to the fact that the overall heat generating region is closer to the cold wall leading to an effective removal of heat. $\overline{Nu}$ calculated for $D_1 = -0.45$ and 0.45

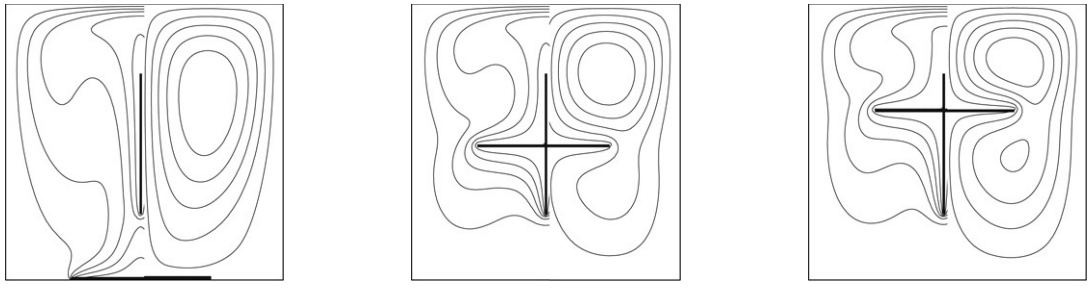

(a) $\Psi_{\max} = 26.4772$. (b) $\Psi_{\max} = 21.9350$. (c) $\Psi_{\max} = 18.4320$.

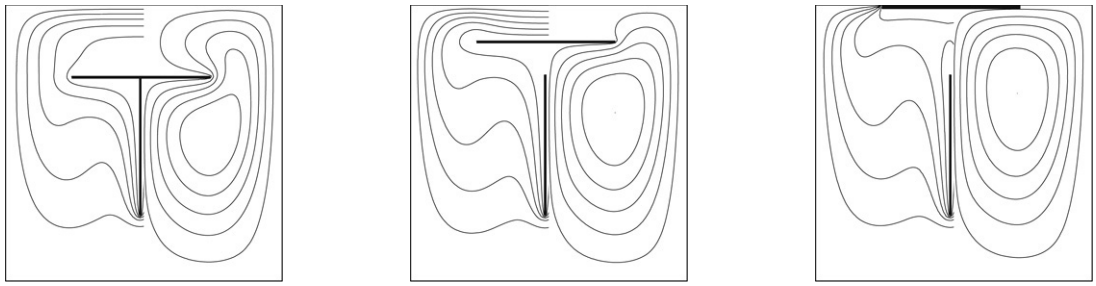

(d) $\Psi_{\max} = 15.6478$. (e) $\Psi_{\max} = 15.8220$. (f) $\Psi_{\max} = 18.5918$.

Fig. 3. Isotherms and streamlines for ITBC, when $D_2 = 0$ and $D_1 = -0.5, 0.0, 0.125, 0.25, 0.375, 0.5$.

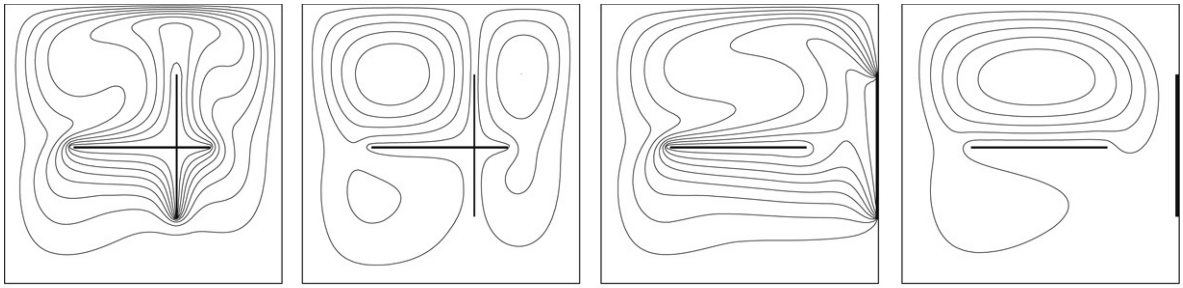

(a) (b) $\Psi_{max} = 26.9355$ (c) (d) $\Psi_{max} = 29.1792$

Fig. 4. Isotherms and streamlines for ITBC when $D_1 = 0$ and $D_2 = 0.125$ and 0.5.

supports this fact. A similar trend was noticed by Dagtekin and Oztop [15] in their study of natural convection in a cavity with two heated partitions mounted on the bottom wall.

Fig. 4 shows the isotherms and streamlines for $D_1 = 0$ and positive values of D_2 for vertical plate movement. It is clear that as D_2 increases from zero, the right convection cell gets suppressed gradually and the anti-clockwise rotating left convection cell starts filling the entire cavity. A close look at the isotherms and streamlines for the case $D_2 = 0.5$ indicates that the role of horizontal plate is more in inducing convection. $\overline{Nu}$'s for different values of D_2 are shown in Fig. 6(b). As D_2 increases from zero, the symmetry in the flow pattern is disturbed and two cells with different strengths are produced. This causes reduction in the overall heat transfer rate though there is an increase in $\Psi_{\max}$. When the plate moves closer to the right cold wall the conduction effect becomes significant and in turn results in higher $\overline{Nu}$ which is similar to the vertical movement of the horizontal plate. But in the extreme wall mounted case ($D_2 = 0.5$), $\overline{Nu}$ again drops due to the formation of a comparatively weak anti-clockwise rotating cell filling the entire cavity.

In order to have a complete understanding, we have plotted the flow characteristics in Fig. 5 corresponding to the extreme cases when both the plates are wall mounted. The absence of any barrier to the flow in the cavity and the shape of isotherms clearly indicate the development of a strong convection pattern with $\overline{Nu}$ as high as 13.46 for

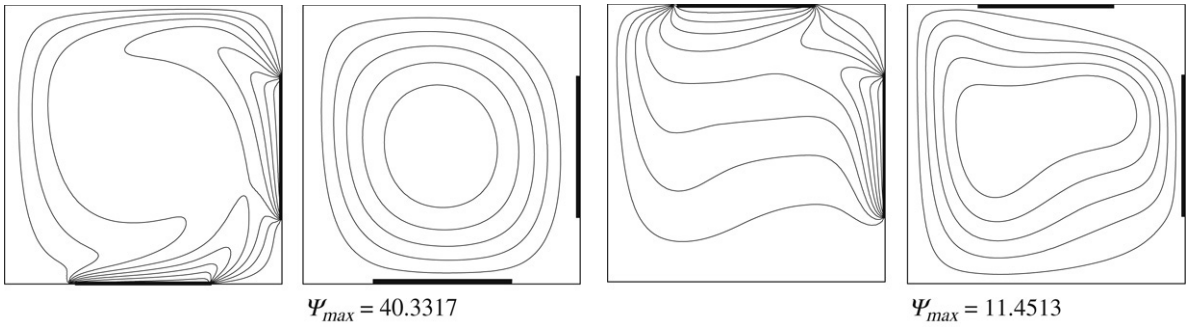

(a) $D_1 = -0.5$ and $D_2 = 0.5$. (b) $D_1 = D_2 = 0.5$.

Fig. 5. Isotherms and streamlines for ITBC.

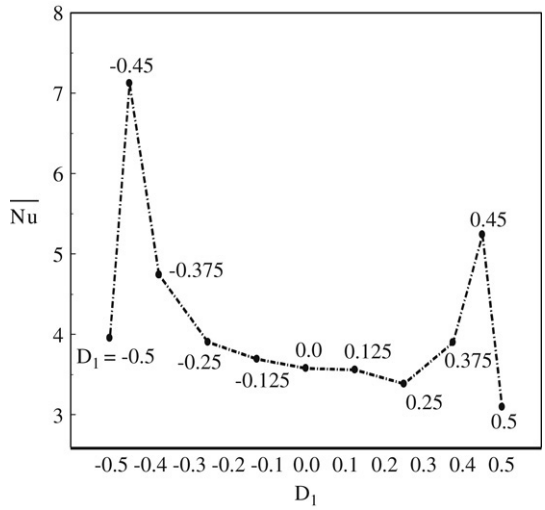

Fig. 6(a). $\overline{Nu}$ for ITBC when $D_2 = 0$ and different values of D_1.

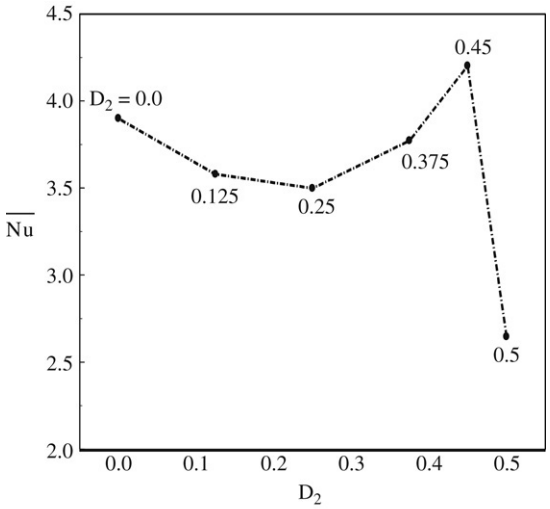

Fig. 6(b). $\overline{Nu}$ for ITBC when $D_1 = 0$ and different values of D_2.

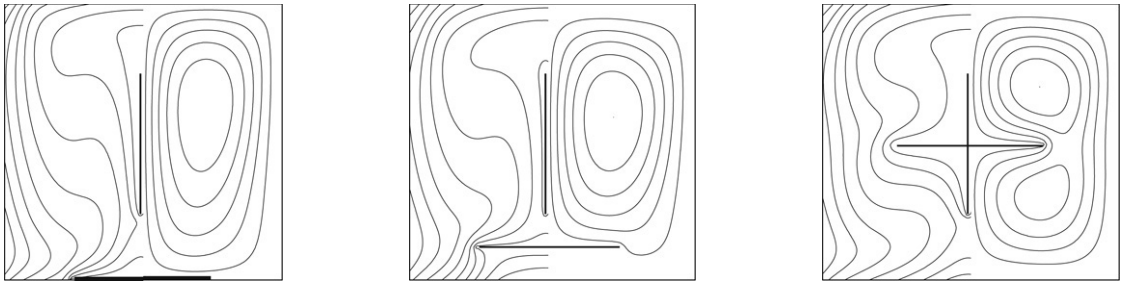

(a) $\Psi_{\max} = 16.4105$. (b) $\Psi_{\max} = 15.5248$. (c) $\Psi_{\max} = 11.54261$.

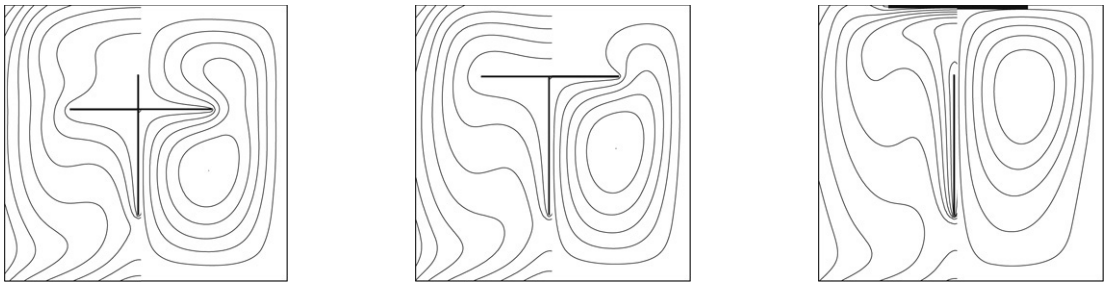

(d) $\Psi_{\max} = 11.0528$. (e) $\Psi_{\max} = 12.1716$. (f) $\Psi_{\max} = 12.9316$.

Fig. 7. Isotherms and streamlines for IFBC when $D_2 = 0$ and $D_1 = -0.5, -0.375, 0.0, 0.125, 0.25, 0.5$.

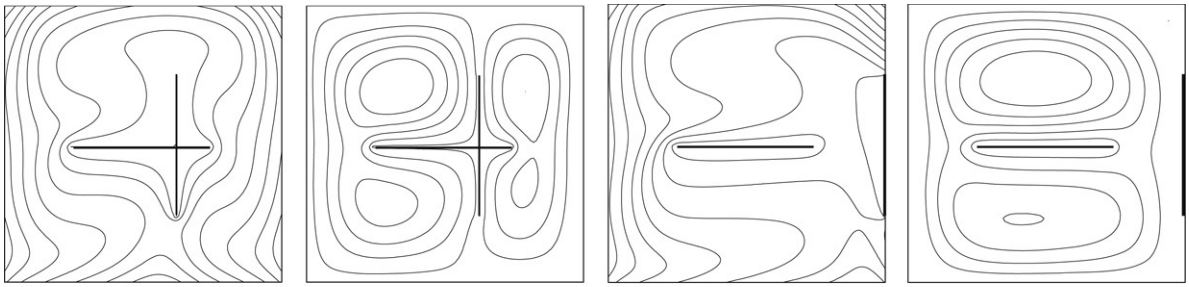

(a) (b) $\Psi_{max} = 12.4413$ (c) (d) $\Psi_{max} = 18.4068$

Fig. 8. Isotherms and streamlines for IFBC when $D_1 = 0$ and $D_2 = 0.125$ and 0.5.

$D_1 = -0.5$ and $D_2 = 0.5$. But a completely different trend is observed for the case $D_1 = D_2 = 0.5$. Though there is no mechanical barrier as in the previous case, the presence of stable thermal stratification in the core region of the cavity suppresses the growth of convection very much. A lowest $\overline{Nu} = 1.90$ is observed for this case. We also find that $\overline{Nu}$'s for all one plate wall mounted case lie between the above two extreme $\overline{Nu}$'s, i.e., as far as the wall mounted cases are concerned, maximum and minimum heat transfer rates can occur only when both the plates are wall mounted.

3.2. Isoflux boundary condition (IFBC)

A uniform outward heat flux applied at the cavity walls makes the isotherms to move away from the plates and get scattered. Since the streamlines corresponding to IFBC fill the cavity more evenly than those corresponding to ITBC (see Figs. 7 and 8), the cavity is made more thermally active for all values of D_1 and D_2. IFBC arrests the formation of thermal boundary layer as in ITBC when one of the plates comes closer to the cavity walls. The isotherms and streamlines corresponding to $D_1 = D_2 = 0$ are shown in Fig. 7(c). We observe a stronger secondary eddy at the cavity bottom of approximately the same strength as that in the top in contradiction to the situation in ITBC. Moreover we observe a reduction in the strength of streamlines $\Psi_{\max}$ compared to ITBC due to the lack of crowding of isotherms.

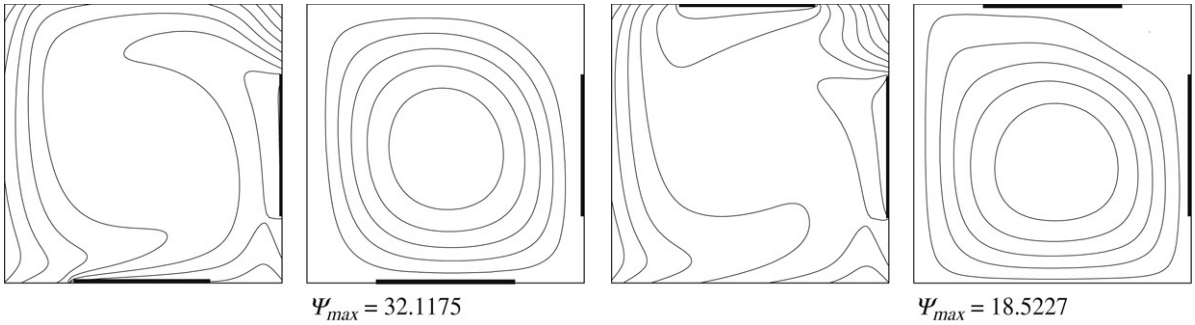

(a) $D_1 = -0.5$ and $D_2 = 0.5$. (b) $D_1 = D_2 = 0.5$.

Fig. 9. Isotherms and streamlines for IFBC

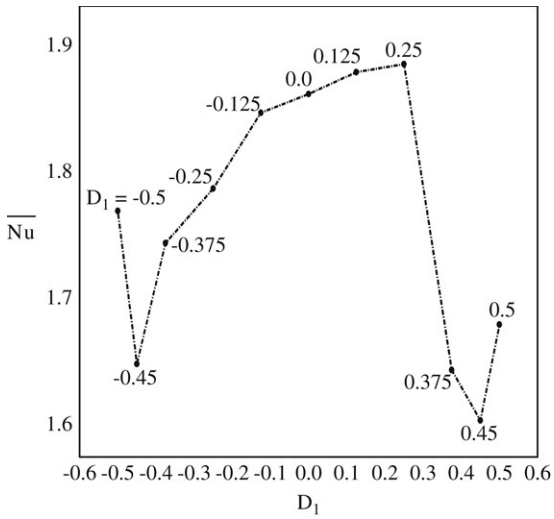

Fig. 10(a). $\overline{Nu}$ for IFBC when $D_2 = 0$ and different values of D_1.

It is also noticed that as the horizontal plate moves upwards in the core region the primary eddy migrates to the bottom of the horizontal plate (even when $D_1 = 0.125$) at a faster rate. This augments the local wall heat transfer at the walls adjacent to the bottom cell and hence increases $\overline{Nu}$ (see Fig. 10(a)) though there is a decrease in $\Psi_{\max}$. The patterns of temperature and streamfunction distribution for different values of D_2 are displayed in Fig. 8. The average Nu for various locations of the plates is shown in Figs. 10(a) and 10(b). A monotonic increase in $\overline{Nu}$ is noticed as the vertical plate moves closer to the wall in contrast to the behaviour in ITBC. We also note a substantial drop in $\overline{Nu}$ as the horizontal plate comes closer to the cavity boundary. The flow characteristics corresponding to both plates wall mounted cases (Fig. 9) show more well developed rotating patterns for $D_1 = D_2 = 0.5$ compared to ITBC.

4. Conclusion

Buoyancy convection in a square cavity induced by two mutually perpendicular heated thin plates is investigated numerically under two different temperature boundary conditions. The following conclusions are drawn. Unlike the ITBC case the convection cell of the IFBC case fills the entire cavity but with lesser strength. It is found that the excess heat energy can be removed efficiently if one of the plates lies away from the core region for ITBC and within the core region for IFBC. In the case of ITBC an upward horizontal plate movement and the vertical plate movement away from the cavity center in the core region both produce a decrease in overall heat transfer whereas in the base of IFBC they both increase overall heat transfer. In the case of ITBC, overall heat transfer shoots up when one of the plates comes close to a cavity wall due to the formation of a thermal boundary layer and overall heat transfer suddenly drops when the plate comes into contact with the cavity wall.

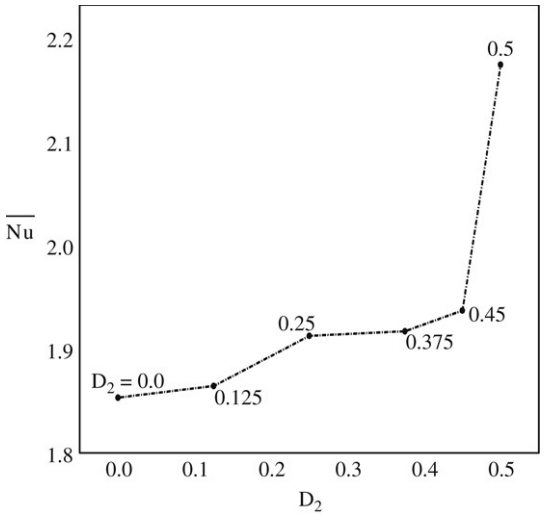

Fig. 10(b). $\overline{Nu}$ for IFBC when $D_1 = 0$ and different values of D_2.

References

[1] G. de Vahl Davis, Laminar natural convection in an enclosed rectangular cavity, Int. J. Heat Mass Transf. 11 (1968) 1675–1693.
[2] A. Bejan, Convection Heat Transfer, Wiley, New York, 1984.
[3] Z.Y. Zhong, K.T. Yang, J.R. Lloyd, Variable property effects in laminar natural convection in a square enclosure, ASME J. Heat Transf. 17 (1985) 133–138.
[4] S. Ostrach, Natural convection in enclosure, ASME J. Heat Transf. 110 (1988) 1175–1190.
[5] S. Saravanan, P. Kandaswamy, Natural convection in low Prandtl number fluids with a vertical magnetic field, ASME J. Heat Transf. 122 (2000) 602–606.
[6] S.M. Bajorek, J.R. Lloyd, Experimental investigation of natural convection in partitioned enclosures, ASME J. Heat Transf. 104 (1982) 527–532.
[7] M. Ciofalo, T.G. Karayiannis, Natural convection heat transfer in a partially or completely — Partitioned vertical rectangular enclosure, Int. J. Heat Mass Transf. 34 (1991) 167–179.
[8] R.L. Frederick, Natural convection in an inclined square enclosure with a partition attached to its cold wall, Int. J. Heat Mass Transf. 32 (1989) 87–94.
[9] X. Shi, J.M. Khodadadi, Laminar natural convection heat transfer in a differentially heated square cavity due to a thin fin on the hot wall, ASME J. Heat Transf. 125 (2003) 624–634.
[10] E.K. Lakhal, M. Hasnaoui, E. Bilgen, P. Vasseur, Natural convection in inclined rectangular enclosures with perfectly conducting fins attached on the heated wall, Heat Mass Transf. 32 (1997) 365–373.
[11] J.M. House, C. Beckermann, T.F. Smith, Effect of centered conducting body on natural convection heat transfer in an enclosure, Numer. Heat Transf. Part A 18 (1990) 213–225.
[12] S. Saravanan, P. Kandaswamy, Free convection in an inclined enclosure with internal heat generation, in: Proc. 4th Asian Comp. Fluid Dyn. Conf., Mianyang, 2000, pp. 664–669.
[13] M. Keyhani, L. Chen, D.R. Pitts, The aspect ratio effect on natural convection in an enclosure with protruding heat source, ASME J. Heat Transf. 113 (1991) 883–891.
[14] H.F. Oztop, I. Dagtekin, A. Bahloul, Comparison of position of a heated thin plate located in a cavity for natural convection, Int. Commun. Heat Mass Transfer 31 (2004) 121–132.
[15] I. Dagtekin, H.F. Oztop, Natural convection heat transfer by heated partitions within enclosure, Int. Commun. Heat Mass Transfer 28 (2004) 823–834.
[16] G.R. Ahmed, M.M. Yovanovich, Numerical study of natural convection from discrete heat sources in a vertical square enclosure, AIAA J. Thermophys. 6 (1992) 121–127.
[17] M.M. Ganzarolli, Natural convection in a rectangular enclosure heated from below and symmetrically cooled from the sides, Int. J. Heat Mass Transf. 38 (1995) 1063–1073.
[18] M.A.R. Sharif, T.R. Mohammad, Natural convection in cavities with constant flux at the bottom wall and isothermal cooling from the sidewalls, Int. J. Thermal Sci. 44 (2005) 865–878.
[19] E. Papanicolaou, Y. Jaluria, Mixed convection from simulated electronic components at varying relative positions in a cavity, ASME J. Heat Transf. 116 (1994) 960–970.
[20] T. Icoz, Y. Jaluria, Design of cooling systems for electronic equipment using both experimental and numerical inputs, ASME J. Electron. Packaging 126 (2004) 465–471.
[21] K.R. Rajagopal, M. Ruzicka, A.R. Srinivasa, On the Oberbeck–Boussinesq approximation, Math. Models Methods Appl. Sci. 6 (8) (1996) 1157–1167.